Journal of Nuclear Materials 396 (2010) 208–217

Contents lists available at ScienceDirect

Journal of Nuclear Materials

journal homepage: www.elsevier.com/locate/jnucmat

Influence of fission products on ruthenium oxidation and transport in air ingress nuclear accidents

N. Vér *, L. Matus, M. Kunstár, J. Osán, Z. Hózer, A. Pintér

Hungarian Academy of Sciences KFKI Atomic Energy Research Institute, H-1525 Budapest 114, P.O. Box 49, Hungary

ARTICLE INFO

Article history:
Received 6 August 2009
Accepted 10 November 2009

ABSTRACT

In separate effect tests at 1000–1200 °C Ru oxidation rate and content of Ru in escaping air flow have been studied with special emphasis on effects of other fission product elements on the Ru oxidation and transport. The results showed that in the decreasing temperature section (1100–600 °C) most of the RuO_3 and RuO_4 (≈95%) decomposed and formed RuO_2 crystals; while the partial pressure of RuO_4 in the escaping air was in the range of 10^{-6} bar. The re-evaporation of deposited RuO_2 resulted in about 10^{-6} bar partial pressure in the outlet gas as well. Measurements demonstrated the importance of surface quality in the decreasing temperature area on the heterogeneous phase decomposition of ruthenium oxides to RuO_2. On the other hand water or molybdenum oxide vapour in air appears to decrease the surface catalyzed decomposition of RuO_x to RuO_2 and increases RuO_4 concentration in the escaping air. High temperature reaction with caesium changed the form of the released ruthenium and caused a time delay in appearance of maximum concentration of ruthenium oxides in the ambient temperature escaping gas, while reaction with barium and rare earth oxides extended Ru escape from the high temperature area.

© 2009 Elsevier B.V. All rights reserved.

1. Introduction

Earlier severe accident studies considered that mainly gaseous and volatile fission products would be released from the damaged fuel during reactor accidents and some noble metals like ruthenium would not be released to any significant extent [1]. The importance of potential ruthenium release was considered only in the vitrification phase of spent fuel processing [2]. Further investigations and the Chernobyl accident indicated that under air ingress conditions the metallic ruthenium can be oxidised and radioruthenium in form of gaseous RuO_3 and RuO_4 could be released in high degree (≈100%) from the damaged fuel [3].

Ruthenium has significant fission yield (about 8% of the fission product inventory [4]). Approximately 70% of fission product ruthenium is in stable isotope form. Through its isotopes ^{103}Ru ($t_{1/2} = 39.3$ days) and ^{106}Ru ($t_{1/2} = 369$ days) ruthenium is radiologically important in both a short and a long term. The amount of produced ruthenium in fuel increases with burn-up and with fuel enrichment in ^{235}U. Moreover its content is greater in mixed oxides (MOX) fuel than in UO_2 fuel [5]. As a consequence in the future the ruthenium amount formed in fuel will rise with optimizing of fuel performance.

In spite of the many experiments devoted to ruthenium release phenomena, prediction of consequences of severe accidents with air ingress is still a challenge and needs further model development in severe accident codes. One work package (WP) of the source term topic of the EU 6th Framework Network of Excellence project SARNET is producing and synthesizing information on ruthenium release and transport with the aim of validating or improving the corresponding modelling in the European ASTEC severe accident analysis code [6].

Several experiments performed in Canada (at AECL) and France (at CEA) were devoted to provide data on fission product release, among them ruthenium, from irradiated fuel rods under severe accident conditions.

In the AECL test series the kinetics of fission-product releases from bare (MCE-1 tests) and from Zircaloy-sheathed segments of CANDU fuel (HCE3 tests) were measured in inert and oxidising conditions. In MCE-1 tests at 1700–2077 °C by changing from inert to oxidising conditions, the kinetics of the Ru release was found much faster than the I or Cs releases which was considered to be consistent with the formation of volatile ruthenium oxides [7]. In HCE3 series two high-temperature steam tests (H01, 1930 °C and H03, 1840 °C) showed a release of ≈4% of Ru. An air test at 1890 °C (H02) showed the greatest release of Ru (≈90%) for a sheathed sample with two end-caps. Ruthenium release began at significant period of time (>2000 s) after oxidative release of volatile fission products. This delay was supposed to be due to the competition among Zircaloy, UO_2 and Ru for oxygen [8].

However some experiments performed in the frame of VERCORS programme at CEA showed relative high release of ruthenium not

---

* Corresponding author. Tel.: +36 1 3922222x1310; fax: +36 1 3959293.
E-mail address: nver@aeki.kfki.hu (N. Vér).

0022-3115/$ - see front matter © 2009 Elsevier B.V. All rights reserved.
doi:10.1016/j.jnucmat.2009.11.008

only in air atmosphere, but also in steam (65% in HT2 test) and even steam-hydrogen atmospheres (28% in RT6 test) as a consequence of oxidising conditions associated with high burn-up of the investigated UO_2 fuel elements (48GWd/t and 72GWd/t, respectively) [6,9]. Analyses of ruthenium deposits along the VERCORS loop confirmed the existence of volatile ruthenium oxide forms in oxidising conditions, and an increase of their fraction on high burn-up UO_2 fuels and on MOX fuels.

In experiments carried out at VTT formation and transport of volatile ruthenium oxides was studied by exposing RuO_2 powder to diverse oxidising atmospheres at 827–1427 °C or by injecting gaseous RuO_4 into the facility in similar conditions [10,11]. The authors found that the fraction of gaseous ruthenium of all ruthenium transported through the facility was at its highest level at 1027 °C (≈40% in dry air flow) although the release rate continued to increase as the temperature of the furnace was increased. At 1227 °C the transport of gaseous ruthenium was dramatically decreased (0.1–0.8%). The authors supposed that at higher temperatures (1227 °C and above) the gaseous ruthenium release was almost limited to the revaporisation of deposited RuO_2 and ruthenium transport took place almost entirely as aerosol particles. The fraction of released ruthenium transported as RuO_2 particles was found increased with reactor temperature ranging from less than 1% at 827 °C to about 35% at 1427 °C. Gaseous RuO_3 produced during the oxidation of the sample was assumed for the main source of both RuO_2 particles and large amount of deposition within the facility where temperature decreases to about 800 °C. RuO_4 decomposition at about 100–150 °C was experienced to be enhanced by stainless steel surface (compared to alumina), and on stainless steel surface by deposited RuO_2 particles.

Recently more experiments were performed at IRSN to investigate ruthenium behaviour under conditions prevailing in the containment in a hypothetical severe accident with the aim of improving assessment of potential radionuclide release into the environment. From the results of RuO_4(g) stability experiments the half-life time of RuO_4(g) was found about 5 h at 90 °C, and 9 h at 40 °C, in the presence of steam. No specific affinity of RuO_4(g) with investigated surfaces (stainless steel and steel covered with epoxy paint) was found, while the humidity and the presence of RuO_2 deposits was supposed to play a catalytic role in the decomposition process [12]. XPS results proved that Ru was present on the surface of the deposits as an oxyhydroxide species of Ru(IV) [13]. Possible revolatilisation of RuO_2 deposited on containment inner walls or ruthenium species present in the aqueous phase (sump) by oxidising medium induced by air radiolysis in the reactor containment building were experimentally evidenced [14,15].

The RUSET (RUthenium SEparate Effect Test) experimental program was launched in order to investigate ruthenium high temperature oxidation and transport through a decreasing temperature area in air stream to understand the formation and possible behaviour of ruthenium oxides in the primary circuit during an air ingress accident. These simplified experiments were aimed to investigate the effects of other fission products on the Ru oxidation and release. New data from the RUSET measurements provide complementary information to the results of the above listed experiments and can help in interpretation of integral tests and in model development to base estimations on realistic assumptions about the chemical nature of the radionuclides.

2. Experimental

2.1. Oxidation setup and procedure

High temperature conditions were established in a vertical furnace. The furnace had three independently heated stages and a joint microprocessor control resulting 150 mm long stable temperature section with about 1–2 °C accuracy. The reaction chamber was a quartz tube with a larger diameter part at the middle containing the test mixture. The experimental device is shown schematically in Fig. 1.

The upper end of furnace area was closed with a 65 mm long annular ceramic cone at the outlet section. The aim of this arrangement was to get a reproducible decreasing temperature stage for the determination of precipitation extent as a function of temperature. The decreasing temperature scale was determined by thermocouples.

Samples consisted of solid state mixtures of the investigated fission product (FP) elements and metallic ruthenium powder in ZrO_2 matrix. The applied composition of inactive fission product components was similar to that used in the SASCHA experiments at FZK representing a 44 MWd/kgU burn-up fuel (see Table 1) [16].

With an air flow rate of 171 cm^3/min (NTP) the evaporation of Ru was fast enough to result in equilibrium partial pressures for ruthenium oxides at beginning of experiments. Isothermal experiments were performed at 1000, 1100 and 1200 °C. During the tests air injection was started when sample in the furnace reached the required temperature.

The released ruthenium was collected in two places:

- in an inner quartz tube (185 mm) placed into the outlet tube of reaction chamber to determine the amount of deposited RuO_2 in the decreasing temperature area and,
- in an ambient temperature absorber solution (1 M NaOH–0.05 M NaOCl) at final outlet air to quantify the gaseous ruthenium oxide components in the outlet gas after cooling down. To improve the efficiency of absorption the absorber solution was cooled in ice bath as suggested by Larsen and Ross [17].

Both the inner quartz tube and the absorber solution were changed at the same time to assess the RuO_x escape from the high temperature area in time. Sampling frequency was 60 min at 1000 °C and 30 min at 1100 °C furnace temperature.

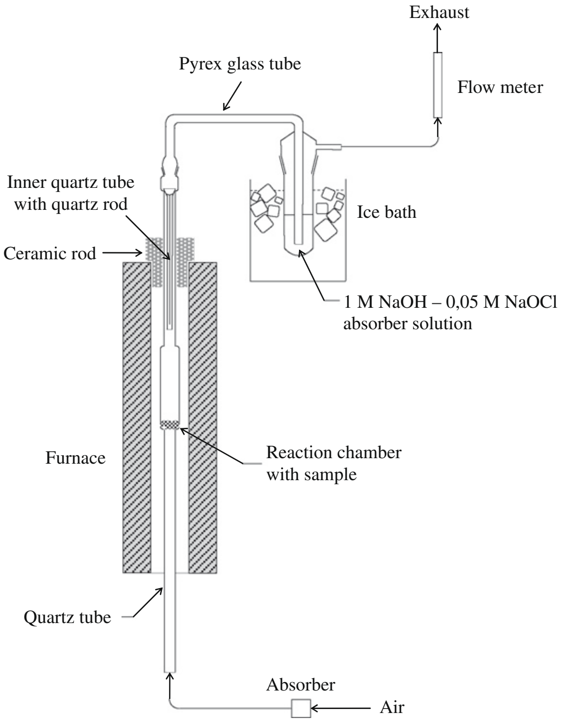

Fig. 1. Experimental set-up.

Table 1
Composition of inactive fission product species used in the SASCHA experiments at FZK [16] representing a middle burn-up (44 MWd/kgU) fuel.

Compounds	Quantity for 100 g charge (mg)
CsI	71.3
Cs_2CO_3	404.8
Mo	394.8
Se	5.9
Sb	2.5
Cd	13.2
Te	69.6
Sn	7.0
Ag	7.4
Ru	502.0
Nd_2O_3	1111.1
CeO_2	405.8
$BaCO_3$	436.7
ZrO_2	570.0

To understand chemical reactions in the decreasing temperature outlet area and thermo chromatographic effects, a quartz rod (170 mm with 2 mm diameter) was placed into the first applied quartz inner tube. The surfaces of quartz rods were investigated using micro-beam X-ray fluorescence (μ-XRF) technique in order to determine the axial distribution of the deposited inactive simulated fission elements with acceptable resolution. Besides quartz fibre filters applied in the inlet of gas absorber or at the top of reaction chamber outlet tube were studied by Philips SEM 505 scanning electron microscope (SEM) and LINK AN 10/55 S type electron beam microanalyser (EDX) to find RuO_2 aerosol formation.

2.1.1. Tests with pure ruthenium and with a set of main fission products

In every case 1 g ZrO_2 with ≈5 mg Ru powder or with mixtures of fission product elements containing ≈5 mg Ru (for composition see Table 1) was filled as a charge into the reaction chamber. At two tests 100 mg UO_2 were given to the charge of ZrO_2 and FP elements. In these first experiments (signed with ‘a’) the absorber solution was 1 M HCl and only one inner quartz tube was used, i.e. RuO_2 was not removed from the decreasing temperature area during the measurement (several hours).

In all later tests the absorber was alkaline hypochlorite solution and both the inner quartz tube and the absorber solution were changed at the same time. Experimental conditions for tests with metallic Ru powder without or with removing RuO_2 from the decreasing temperature area at regular intervals are summarized in Table 2.

Table 2
Experimental conditions for tests with pure metallic Ru powder or Ru with other FPs in ZrO_2 matrix without (signed with ‘a’) or with removing RuO_2 from the decreasing temperature area (i.e. using one inner quartz tube during the full duration of measurement or changing inner quartz tubes with absorber solutions at the same time).

Experiment	Charge	Temperature (°C)	Remarks
a4	Ru	1100	–
a5	Ru	1100	Air stream: 300 cm^3/min
a6	Ru	1000	–
a7	Ru	1100	SS inlet
a8	Ru	1200	–
a9, a12	Ru	1100	Wet air
a11	Ru	1100	Dry, then wet argon
a17	Ru + FPs	1100	Wet air
a18	Ru + FPs + UO_2	1100	Wet air
a19	Ru + FPs + UO_2	1100	–
7	Ru	1000	–
8, 33	Ru	1100	–

2.1.2. Tests with Mo–Ru–Rh–Pd alloy

Ruthenium appears in irradiated UO_2 in form of small alloy precipitations together with Mo, Rh, Pd and Tc (white inclusions) [18]. In this test series differences between ruthenium evaporation rates from pure ruthenium metal and from Mo–Ru–Rh–Pd alloy (as a simulant for white inclusions) were investigated. The chemical composition of the alloy (Mo 47%/Ru 27%/Rh 7%/Pd 19% by weight) was determined based on literature data for spent PWR fuel with a burn-up of 36.195 MWd/kgU [19]. Experiments were performed using 1 g ZrO_2 matrix with ≈18.52 mg powdered alloy (containing ≈5 mg Ru), moreover with other inactive fission product components (for the applied concentrations see Table 1) as well. The test parameters are compiled in Table 3. Note: in these tests the concentration of Mo in the charge was 2.2 times of that in the SASCHA experiments.

2.1.3. Tests with selected groups of fission products

To investigate the effects of several fission product components on the formation, transport and decomposition behaviour of ruthenium oxides in high temperature air stream, they were divided into four characteristic groups:

- Ru + metals (Mo, Se, Sn, Ag, Sb, Cd, Te).
- Ru + Ba compounds ($BaO/BaCO_3$).
- Ru + rare earth oxides (Nd_2O_3, CeO_2).
- Ru + Cs compounds (CsI, Cs_2CO_3).

In these tests 1 g ZrO_2 with a group of fission product elements containing ≈5 mg Ru was filled as a charge into the reaction chamber.

Formation of Cs_2RuO_4 can increase the volatility of Ru [20] and change the transport and decomposition mechanisms of it in the decreasing temperature area. For this reason it is of primary importance to understand the high temperature interaction of ruthenium oxides with caesium compounds. Solid state mixture of Ru with CsI and Cs_2CO_3 at mol ratios of stoichiometric, sub- and super-stoichiometric according to Cs_2RuO_4 were oxidised in high temperature air stream. In every case ≈5 mg Ru with different amounts of caesium compounds (Cs:Ru = 0.56; 1.00; 1.51; 2.01 and 4.03) in 1 g ZrO_2 matrix was used as a charge. The relative amounts of CsI and Cs_2CO_3 were the same in every sample according to Table 1.

While the volatility of fission product caesium is much higher both in reducing and oxidising conditions than that of ruthenium, Cs will be deposited on the cold surfaces in the reactor cooling system (RCS) earlier than ruthenium oxides during a severe accident scenario [7,8]. To investigate the effect of Mo- and Cs-oxides deposition in the decreasing temperature area on the decomposition of ruthenium oxides, in two experiments (Nos. 24 and 30) first the sampling inner quartz tubes were covered by evaporation of Mo powder or of CsI–Cs_2CO_3 mixture in air stream from the usual ≈1 g ZrO_2 and then these tubes were used in a second measurement with pure metallic Ru powder in the charge.

The experimental matrix for tests with selected groups of fission product elements is summarized in Table 4.

Table 3
Experimental matrix of tests with Mo–Ru–Rh–Pd alloy.

Experiment	Charge	Temperature (°C)	Remarks
2	Alloy	1000	–
5	Alloy + FPs	1000	–
1, 3	Alloy	1100	–
4, 6	Alloy + FPs	1100	–

Table 4
Experimental conditions for tests with selected groups of fission product elements.

Experiment	Charge	Temperature (°C)	Remarks
18	Ru + Mo group	1000	–
15, 17	Ru + Mo group	1100	–
24	Ru	1100	Mo covered inner tubes
20	Ru + Ba compounds	1000	–
13	Ru + Ba compounds	1100	–
21	Ru + rare earth oxides	1000	–
14	Ru + rare earth oxides	1100	–
19	Ru + Cs compounds	1000	Cs:Ru = 0.56
11, 22	Ru + Cs compounds	1100	Cs:Ru = 0.56
32	Ru + Cs compounds	1100	Cs:Ru = 1.00
35	Ru + Cs compounds	1100	Cs:Ru = 1.51
31	Ru + Cs compounds	1100	Cs:Ru = 2.01
34	Ru + Cs compounds	1100	Cs:Ru = 4.03
30	Ru	1100	Cs covered inner tubes

2.2. Determination of ruthenium balance

The total weight of deposited components in a given sampling period (Δm) was measured by weighing the inner quartz tubes before and after their use. Based on numerous pre-experiments to reduce RuO_2 quantitatively to Ru, a heat treatment in 5% $H_2 + N_2$ gas stream at 1100 °C for 5 h proved to be appropriate. The Ru could be dissolved in alkaline hypochlorite solution and this was used directly for spectrophotometric measurements. This reduction process provided reliable results even in the presence of other deposited elements like Mo, Cs and Te.

Ruthenium absorbed or dissolved by alkaline hypochlorite solution (1 M NaOH–0.05 M NaOCl) was measured in septivalent (perruthenate) form at 380 nm [17].

2.3. μ-XRF analysis of deposited elements on quartz rods

During the measurement the surface of quartz rod was scanned through a microscopic X-ray beam generated by a silver-anode fine-focus X-ray diffraction tube. The beam was focused to 80 μm (FWHM) by means of a polycapillary minilens (IfG, Germany). The X-ray tube was operated at 40 kV and 40 mA. The sample was fixed to a computer-controlled sample stage and moved in front of the capillary. Because of the relatively small range of the movement, the original 170 mm long rod was cut into two pieces. The measurements were carried out in 1 mm steps; each point was measured for 100 s. Spectra were recorded by a Si(Li) X-ray detector and the intensities of the characteristic X-ray lines were evaluated by the AXIL code. Mo and Ru were determined using K lines, while Cs, I and Te using L lines. The relative sensitivities for the lines of interest (Mo-Kα, Mo-Lα, Ru-Kα, Ru-Lα, Cs-Lα, I-Lα, Te-Lα) were determined from measurements of thin standard samples of MoO_3, CsBr and ZnTe (Micromatter), as well as a dried droplet prepared on a polypropylene X-ray film from 1 g/l Mo, Ru and Cs standard solutions (Spectrascan, 5 μl each).

3. Experimental results and discussion

The average partial pressure of RuO_x in the high temperature reaction chamber (p_{furnace}) was calculated from the total amount of precipitated ($\Delta m_{\text{precipitated}}$) and absorbed ($\Delta m_{\text{absorbed}}$) ruthenium, while the average partial pressure of RuO_4 in the escaping ambient temperature gas ($p_{\text{outlet air}}$) was calculated from the amount of ruthenium in the absorber solution ($\Delta m_{\text{absorbed}}$) and the volume of gas streamed through during a given sampling period (V_{air}). The temperature values ($t_{\text{equilibrium}}$), which would result the same partial pressures in equilibrium as measured in the escaping gas ($p_{\text{outlet air}}$), were calculated using the following equilibrium equations published in [21]:

$$\text{for process} \quad RuO_2(s) + O_2 \leftrightarrow RuO_4(g)$$

$$\lg K_p = -6219.4/T + 4.2120 - 1.0315 \lg T - 0.0557 \times 10^5\, T^{-2} \tag{1}$$

$$\text{for process} \quad RuO_2(s) + 1/2O_2 \leftrightarrow RuO_3(g)$$

$$\lg K_p = -12968.5/T + 10.1385 - 1.2429 \lg T - 0.1399 \times 10^{-3}\, T + 0033 \times 10^5\, T^{-2} \tag{2}$$

with K_p (atm) and T (K).

3.1. Formation and transport of ruthenium oxides in high temperature air

In the first test series metallic ruthenium powder was oxidised from ZrO_2 matrix mainly at 1100 °C and in an air stream of 171 cm^3/min (NTP).

In a control test for the role of oxygen (No. a11) for 2 h first dry high purity argon, then for 2 h wet argon was streamed through the high temperature (1100 °C) reaction chamber containing 5 mg Ru powder in ZrO_2. Ru appeared neither in the decreasing temperature outlet tube nor in the absorber solution.

The results showed that Ru evaporates in form of RuO_3 and RuO_4. Partial pressures of RuO_x in the high temperature reaction chamber calculated on the basis of the sum of deposited Ru mass and Ru in liquid solution (see Table 5) were in good agreement with the equilibrium partial pressure of $RuO_4 + RuO_3$ system published in [21,22]. This means that both RuO_3 and RuO_4 reached saturated concentration in the furnace (until enough Ru was present in the ZrO_2 matrix), which limited the rate of Ru oxidation.

In the outlet section of furnace between about 1100 and 600 °C RuO_3 and most of the RuO_4 decomposed and formed characteristic deep blue RuO_2 crystals (CVD – chemical vapour deposition). Only 5–10% of ruthenium reached the room temperature samplers during the total experimental time (several hours). In the later phase of tests using one inner quartz tube, i.e. without removing the precipitated RuO_2 from the decreasing temperature area, Ru escapes were coming from the deposited RuO_2 by re-evaporation into the high temperature air resulting in $\approx 10^{-6}$ bar partial pressure in the outlet gas (see Fig. 2). In [23] the authors found that while the ruthenium release rate from the crucible and ruthenium deposition velocity were constant, the RuO_4 transport was likely increasing at the end of measurement. In some cases similar trend can be seen in our measurements (see Fig. 2) probably as a result of increasing re-evaporation rate of RuO_2 deposits in the later phase of the experiments.

The measured partial pressures of RuO_4 in the ambient temperature outlet air (ranged between 10^{-7} and 10^{-5} bar) are higher by several orders of magnitude than the equilibrium value of $RuO_4 + RuO_3$ system ($\approx 10^{-20}$ bar at 25 °C [21]). At higher furnace temperature (No. a8) or at higher air flow rate (No. a5), higher partial pressures of RuO_x appeared in the escaping air (see Fig. 2). This can be attributed to the fact that the rate of (surface/RuO_2 catalyzed) decomposition process of RuO_4 to RuO_2 was not fast enough to follow entirely the equilibrium with the temperature. The temperature values ($t_{\text{equilibrium}}$), which would result the same partial pressures in equilibrium as measured in the escaping gas (calculated according to (1) and (2) equations), showed that the chemical process of RuO_x to RuO_2 stopped at about 600–800 °C (see Table 5), which agree reasonable well with temperatures at the end of RuO_2 deposition determined from the position and thermocouple calibration.

Table 5
Experimental conditions and results of tests with pure metallic Ru powder in ZrO_2 matrix with changing both the inner quartz tube and the absorber solution at the same time.

Main parameters	Sample	Time (min)	V_{air} (dm^3)	Δm (mg)	$\Delta m_{precipitated}$ (mg)	$\Delta m_{absorbed}$ (mg)	$p_{furnace}$ (bar)	$p_{outlet\ air}$ (bar)	$t_{equilibrium}$ (°C)
t = 1000 °C	7-1	60	10.29	4.33	3.29	0.10	8.12E−05	2.28E−06	745.7
Ru	7-2	60	10.29	1.99	1.51	0.05	3.74E−05	1.14E−06	697.0
m_{Ru} = 5.87 mg	7-3	60	10.29	0.97	0.74	0.04	1.86E−05	9.30E−07	683.4
	7-4	120	20.57	0.20	0.15	0.07	2.66E−06	8.40E−07	676.6
t = 1100 °C	8-1	30	5.14	6.04	4.59	0.08	2.24E−04	3.60E−06	779.3
Ru	8-2	30	5.14	0.73	0.55	0.06	2.92E−05	2.64E−06	756.4
m_{Ru} = 5.22 mg	8-3	30	5.14	0.10	0.08	0.01	4.30E−06	6.60E−07	661.0
t = 1100 °C	33-1	30	5.14	5.76	4.38	0.08	2.14E−04	3.60E−06	779.3
Ru	33-2	30	5.14	0.90	0.68	0.05	3.53E−05	2.52E−06	753.0
m_{Ru} = 5.04 mg	33-3	30	5.14	0.09	0.07	0.00	3.40E−06	1.20E−07	562.9

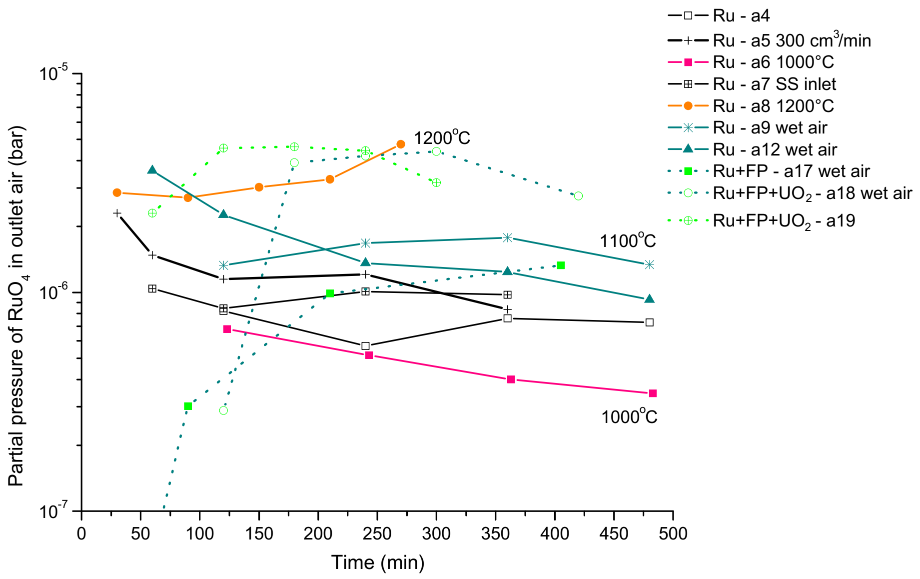

Fig. 2. Partial pressures of RuO_4 in the outlet air in tests using one inner quartz tube during the full measurement duration (i.e. RuO_2 was not removed from the decreasing temperature area as in the later experiments). The temperatures of reaction chamber (air – Ru reaction) were 1100 °C at all experiments except the two tests signed in the plot (1000 and 1200 °C).

However no aerosol formation was found in the given test conditions as in the similar experiments performed at VTT [10,11]. On the quartz fibre filters applied in the inlet of gas absorber or at the top of reaction chamber outlet tube RuO_2 particles could not be seen by SEM and the mass of ruthenium on the filters measured by XRF were lower than 1% of the initial ruthenium mass in the charge. Using quartz fibre filters did not influenced the Ru content in the absorber liquids.

To test the influence of stainless steel (SS) surfaces in the decreasing temperature area on the release of Ru a 0.5 mm thick 170 × 2.6 mm SS plate has been placed into the inner quartz tube (see Fig. 2; No. a7). The RuO_2 precipitation formed on the SS plate was at the same elevation interval as on the quartz tube surface. Even the morphology of precipitation was the same on SS and on quartz surface. The mass of precipitation cannot be weighed, because of the oxidation of SS resulted a substantial mass increase.

Using air with ca 5% steam content, the steam decreased the decomposition of RuO_4 to RuO_2 and resulted in higher RuO_4 partial pressures in the escaping gas ($\approx 1.5–2 \times 10^{-6}$ bar) than in case of dry air (see Fig. 2; Nos. a9 and a12). (In these tests less Ru precipitated in the inner quartz tubes and some more in the tube system going to the sampler unit.) In the VTT experiments [11] at 1027 °C addition of small amount of water vapour into the air flow also increased gaseous RuO_4 transport rate in the outlet air compared to dry condition. (The fraction of gaseous ruthenium of all ruthenium transported through the facility was ≈40% in dry air flow. This fraction increased to ≈70% as the steam volume fraction was increased to at least 10%, and was the highest (≈90%) in air saturated with water vapour at 30 °C.) When steam volume fraction was further increased by them (above 10%), the transport rate decreased below that measured in dry air.

If other fission products were present in the charge (No. a17) the release of Ru started in the beginning of experiments with lower intensity and with certain delay than in tests where the charge was pure Ru powder in ZrO_2. If beside the FP elements 100 mg UO_2 were given to the sample (Nos. a18 and a19) the partial pressure of Ru oxides (after a time) were higher ($\approx 4 \times 10^{-6}$ bar) than in case of Ru powder or Ru powder + fission products. This is probably due to the formation of $BaUO_4$ from $BaCO_3$ and UO_2 at temperatures higher than 1000 °C (see Section 3.3.2.). The delay in escape of Ru was larger at using wet air with ca 5% steam (No. a18) than using dry air (No. a19). After a longer time there is no difference in the escape rate of ruthenium in wet or dry air (see Fig. 2).

3.2. Oxidation and release of ruthenium from Mo–Ru–Rh–Pd alloy

In this test series oxidation and release of ruthenium from Mo–Ru–Rh–Pd alloy as a simulant for white inclusions were investigated. As can be seen from Fig. 3 the oxidation rate of Ru from Mo–Ru–Rh–Pd alloy is about 45% of the evaporation rate of pure

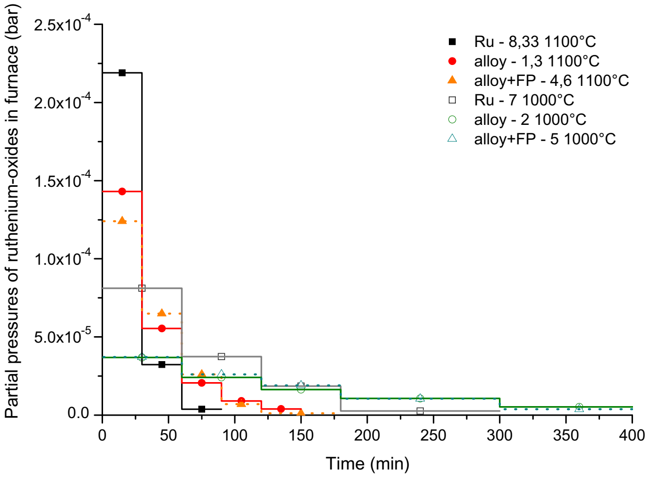

Fig. 3. Partial pressures of RuO_x in the high temperature reaction zone.

Ru at 1000 °C and 55–65% at 1100 °C. This slower reaction rate probably was a result partly of the larger grain size of the powdered alloy as compared to the commercial ruthenium powder and partly of the simultaneous presence of large amounts of Mo, Rh and Pd in the grains as opposed to the other measurements. There were smaller differences in the partial pressures of RuO_x in the high temperature reaction chamber between pure alloy and alloy with other fission product components both at 1000 °C and 1100 °C.

Although there were no significant differences in the partial pressures of RuO_x in the high temperature reaction chamber between pure alloy and alloy with other fission product components at 1000 °C (see Fig. 3), the precipitated amount of Ru was significantly greater in case of pure alloy than in presence of other fission product components after an initial time (60 min) (see Fig. 4). At 1100 °C the amount of Ru leaving the high temperature reaction zone was smaller in the first 30 min, but greater after this initial time in presence of other FPs than at pure alloy oxidation (see Fig. 3). However the amount of precipitated Ru was greater during the whole sampling period in case of pure alloy than in presence of other FPs (see Fig. 4).

Partial pressures of RuO_4 in the ambient temperature escaping air are about one order of magnitude higher in case of alloy or alloy with other FPs than in case of pure Ru (see Fig. 5). While in case of pure alloy concentration of RuO_4 in the outlet air decreased continuously in time, presence of other fission products influenced it and caused a time delay (60–120 min at 1000 °C and 30–60 min at 1100 °C) in appearance of its maximum values.

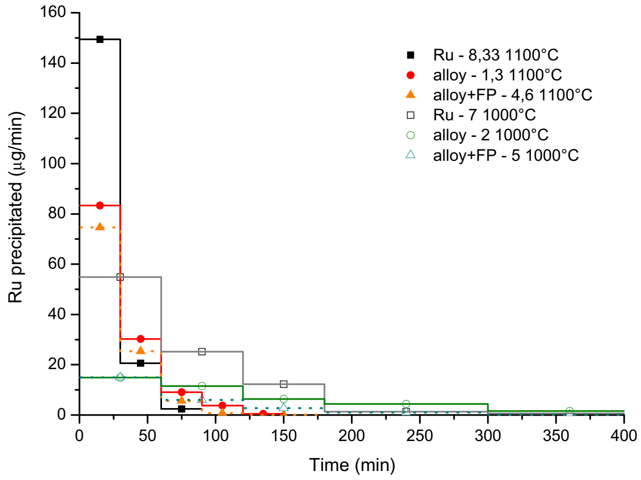

Fig. 4. Amount of Ru precipitated in the decreasing temperature area.

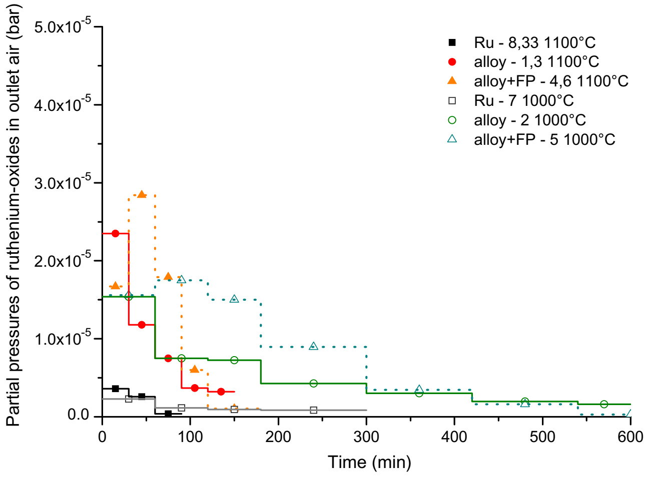

Fig. 5. Partial pressures of RuO_4 in the outlet air.

In presence of other fission product elements there was also a slight time delay in the escaping of Ru from the furnace at both temperatures (see Fig. 3). It suggests that reactions in the high temperature area delayed the release of Ru in the escaping cooled down air (see Sections 3.3.2 and 3.3.3).

At oxidation of Mo–Ru–Rh–Pd alloy the fraction of Ru appeared in the absorber solution was ≈40% at 1000 °C and ≈20% at 1100 °C, while in presence of other FP components these fractions were ≈65% and ≈30%, respectively. In case of pure Ru oxidation only 4–5% of the initial 5 mg Ru reached the absorber solution at 1000 °C, and 2–3% at 1100 °C.

Molybdenum oxides and other FP elements deposited in the inner quartz tube decreased the catalytic effect of quartz tube for decomposition of RuO_x to RuO_2 (for mechanisms see Sections 3.3.1 and 3.3.3) and resulted in nearly one order of magnitude higher RuO_4 partial pressures in the ambient temperature escaping air as in case of pure Ru oxidation.

Because of the high amount of Mo in the investigated alloy the total amount of Ru appeared in absorber solution was about 10 times greater in case of pure alloy (or alloy with other fission products) than in tests conducted with metallic Ru powder. On the other hand the slower escape rate of ruthenium, e.g. because of the bigger grain size of the powdered alloy, the simultaneous presence of high amounts of Mo, Rh, and Pd in the grains, the high temperature reactions with other FPs or the slower oxidation rate at lower temperature (1000 °C) also resulted in higher Ru fraction in the escaping air because of the longer sampling time.

3.3. Delay of ruthenium escape in presence of some fission product elements

The main objectives of these experiments were investigation of effects of four characteristic groups of fission product elements on behaviour of Ru in high temperature air atmosphere and identification of those fission products, which play role in the time delay in appearance of ruthenium oxides in ambient temperature escaping gas and identification of those chemical reactions and/or mechanisms, which causes this delay.

3.3.1. Effects of molybdenum and other metals

The release rate of Ru from the high temperature reaction chamber was slightly lower in case of molybdenum and other metals (Se, Sn, Ag, Sb, Cd, Te) containing mixtures (in tests Nos. 15, 17 and 18) than in case of pure Ru oxidation both at 1000 °C and 1100 °C (see Fig. 6). Above the competition between Ru and Mo oxidation this slightly lower Ru amount measured in case of molybdenum including samples was partly caused by the black uncontrolled deposition on the outlet tube of reaction chamber at the same elevation where ruthenium precipitation occurred in the inner quartz tubes. This phenomenon did not appear in case of other charges and resulted in poorer Ru mass balance.

Molybdenum has its main effect on the surface catalyzed decomposition of ruthenium oxides to RuO_2 in the decreasing temperature area. RuO_2 crystals start to grow on inhomogeneity of the quartz wall and on the formed RuO_2 particles.

Mo oxidizes fairly fast to MoO_3 and in the first minutes after start of air injection polymer $(MoO_3)_n$ appeared as white aerosol (this phenomenon was also experienced in tests with pure Mo–Ru–Rh–Pd alloy). The vapour phase consists predominantly of Mo_3O_9, Mo_4O_{12} and Mo_5O_{15} molecules [24].

In presence of molybdenum in the charge fraction of ruthenium appeared in the absorber solution was about 40% at 1000 °C, and about 13% at 1100 °C, while using MoO_3 covered sampling tubes this part was only ≈7% at 1100 °C (test No. 24). In the vapour phase simultaneously present molybdenum oxides decrease the surface catalyzed decomposition of RuO_x and result in nearly one order of magnitude greater RuO_x partial pressures in the ambient temperature escaping air compared to pure Ru oxidation (see Fig. 7).

As can be seen in Fig. 8 MoO_3 and TeO_2 deposited together in temperature range between 300 and 600 °C. At this area large RuO_2 crystals grew which are usually typical at the higher temperature region. Between 400 and 500 °C stable glasses can form in the MoO_3–TeO_2 system, while at 550–600 °C crystalline or glassy Te_2MoO_7 depending on quenching conditions [25]. The Te peak appeared at about 550 °C. A second Ru peak appeared under 600 °C between 350 and 450 °C.

3.3.2. Influences of barium and rare earth oxides

At temperatures of investigations in the solid state mixtures of ruthenium with barium oxide or rare earth (Nd, Ce) oxides barium ruthenate or rare earth ruthenates can form. These reactions caused elongated Ru escape from the high temperature area (see Fig. 9) and probably also resulted in time delay in appearance of the maximum concentration of RuO_4 in the outlet air (see Fig. 10).

The amount of Ru leaving the furnace and precipitating in the decreasing temperature area was smaller in presence of Ba or Nd and Ce than in case of pure Ru both at 1000 and 1100 °C. On the other hand concentration of Ru in the escaping air was slightly higher at 1000 °C, and after 30 min also at 1100 °C. The slower Ru escape from the high temperature reaction chamber in presence of barium and rare earth oxides resulted in a slightly higher ruthenium fraction in the absorber solution (≈10% both at 1000 and 1100 °C).

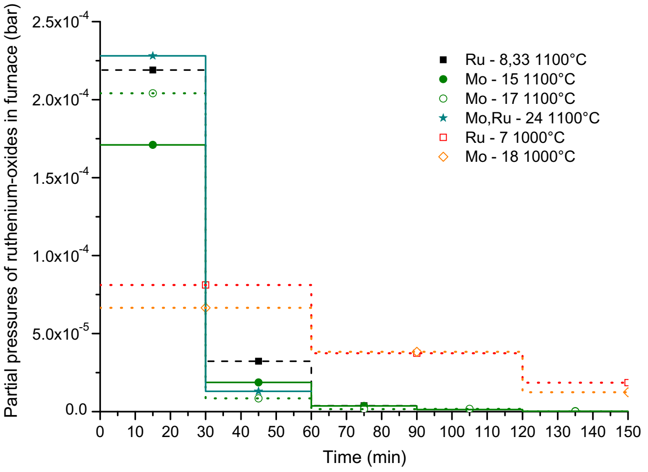

Fig. 6. Partial pressures of ruthenium oxides in furnace (group of Mo and other metals).

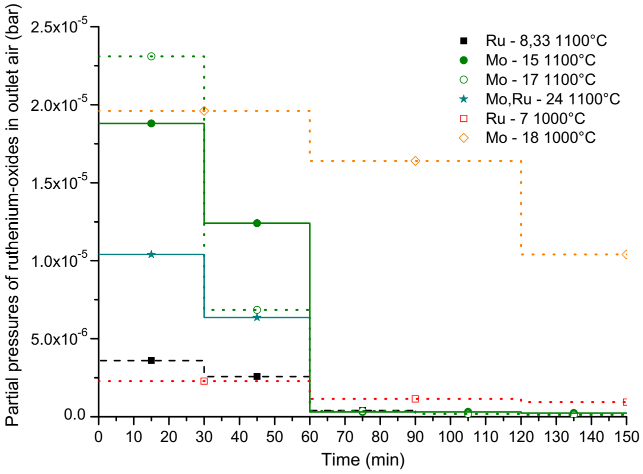

Fig. 7. Partial pressures of ruthenium oxides in outlet air (group of Mo and other metals).

3.3.3. Ruthenium release in presence of caesium compounds

Caesium seems to be the fission product element, which plays main role in time delay in appearance of maximum concentration of ruthenium oxides in the ambient temperature escaping gas.

If Cs was present less than the stoichiometric concentration according to Cs_2RuO_4 in the test mixtures (i.e. at mol ratios of Ru:Cs = 2:1, Ru:Cs = 1:1 and Ru:Cs = 2:3) the maximum concentration of RuO_4 in the outlet air appeared between 30 and 60 min at 1100 °C at sampling frequency of 30 min (see Fig. 11). On the other hand if the sample contained Ru and Cs at mol ratios of 1:2, the fraction of Ru reached the absorber solution was only ≈0.7% during the 90 min sampling period and the concentration of RuO_4 in the ambient temperature outlet air slightly increased in time.

In presence of Cs in the charge the average Ru concentration during the first 30 min in the outlet air was lower than in case of pure Ru. One explanation could be formation of Cs_2RuO_4 in the high temperature reaction chamber. The partial pressure of this compound is much higher ($p_{Cs_2RuO_4} = 1.7428 \times 10^{-3}$ bar [20]) than that of ruthenium oxides ($p_{RuO_3+RuO_4} = 2.4510 \times 10^{-4}$ bar [21]) at 1100 °C. While the deposition mechanism of the Cs_2RuO_4 is condensation, in this case the Ru concentration remaining in the outlet air is much lower ($p_{Cs_2RuO_4} = 2.5931 \times 10^{-25}$ bar at 25 °C [20]) than in case of the surface catalyzed decomposition of ruthenium oxides to RuO_2 ($p_{RuO_4} \approx 10^{-6}$ bar, see Table 5). However interpretation of higher RuO_4 concentration in the escaping gas in the second 30 min at mole ratios of Ru:Cs = 2:1, Ru:Cs = 1:1 and Ru:Cs = 2:3 and the lower RuO_4 concentration at stoichiometric composition (Ru:Cs = 1:2) compared to pure Ru (see Fig. 11) needs further investigations.

In test No. 30 Cs was previously deposited on sampling tubes, and then these tubes were used in a second measurement with pure Ru powder in the charge. By diffusing into the quartz wall, Cs changed the quartz surface feature (decreased its catalytic effect on decomposition of RuO_x to RuO_2) and resulted in nearly one order of magnitude higher RuO_x partial pressures in the ambient temperature escaping air than in case of pure Ru oxidation (see Fig. 11). The fraction of ruthenium appeared in the absorber solution was about 12%. However in [11] the authors found that CsI

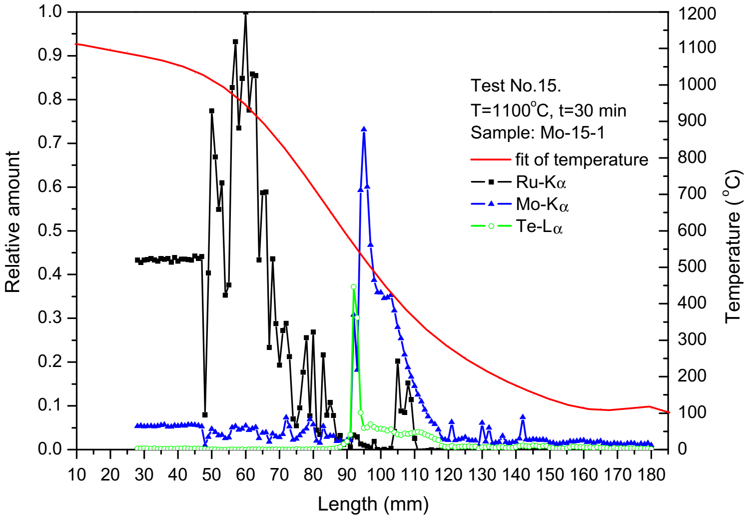

Fig. 8. Axial distribution of deposited elements on quartz rod (sample: Mo-15-1).

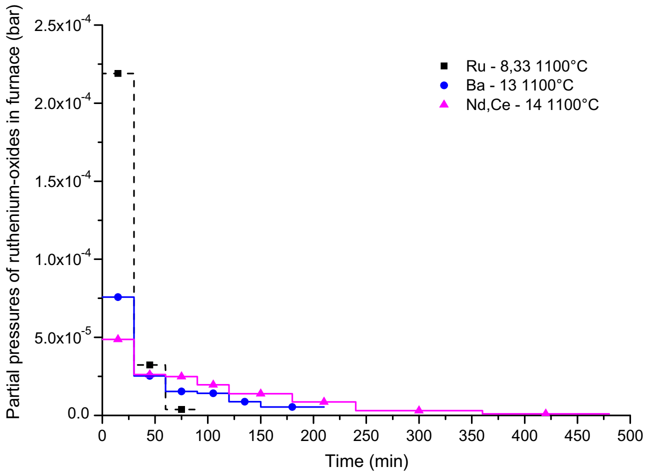

Fig. 9. Partial pressures of RuO_x in high temperature reaction chamber ($BaCO_3$ or Nd_2O_3, CeO_2 containing charges).

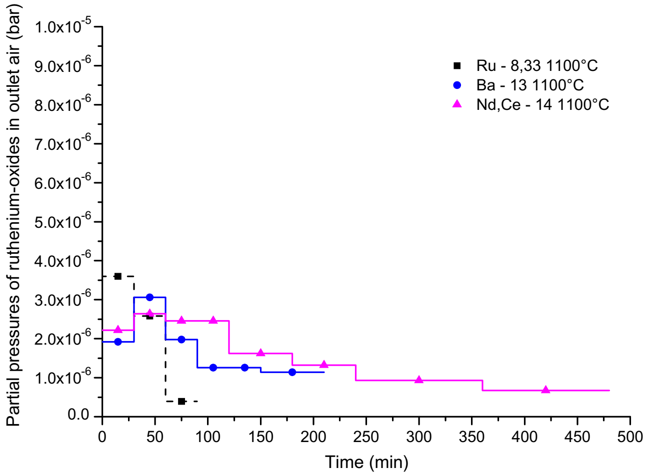

Fig. 10. Partial pressures of RuO_4 in ambient temperature outlet air ($BaCO_3$ or Nd_2O_3, CeO_2 containing charges).

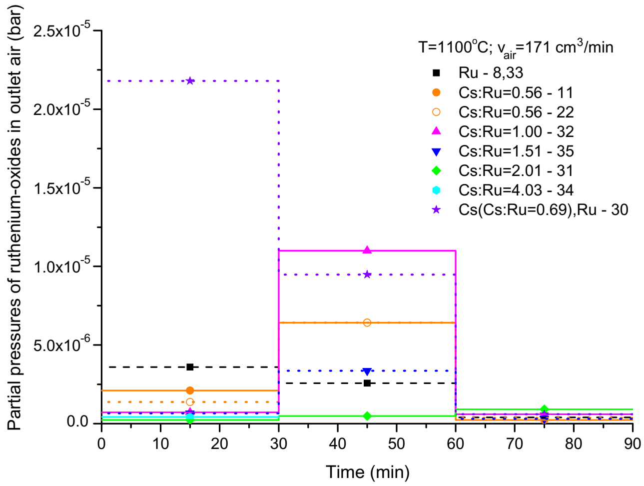

Fig. 11. Partial pressures of ruthenium oxides in outlet air.

powder (mass 1 g) placed inside the alumina tube at location 65–90 cm after the furnace trapped 0.74 mg Ru (3.3% of the injected gaseous RuO_4), and they supposed most likely in the form of Cs_2RuO_4.

An example for results of the μ-XRF measurements can be seen in Fig. 12. If Cs was present in the charge, Ru and Cs deposited together in the decreasing temperature area between 400 and 900 °C, while this phenomenon did not appear if only the inner quartz tube was covered with Cs (see Fig. 13). This probably means that part of the Ru and Cs evaporated from the high temperature reaction chamber in form of some caesium compounds. On the other hand the measured Ru–Cs peaks did not show any constant stoichiometry. Presence of Cs in the charge or on the surface of sampling quartz tubes resulted in ruthenium precipitation at a relatively low temperature region (below 600 °C, while oxidising pure Ru at 1100 °C for 30 min, Ru deposits usually between 600 and 1100 °C). However the reliability of relative amounts of Ru and Cs gained with μ-XRF technique needs further investigations, on the one hand because of diffusion of Cs into the quartz material, on the other hand because of the relative high concentration and inhomogeneity of the investigated elements on the surface of the quartz rods.

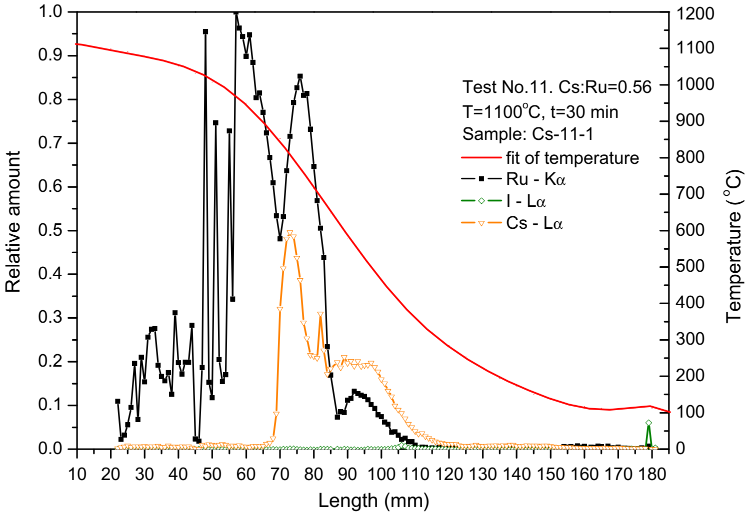

Fig. 12. Axial distribution of deposited elements on quartz rod (sample: Cs-11-1).

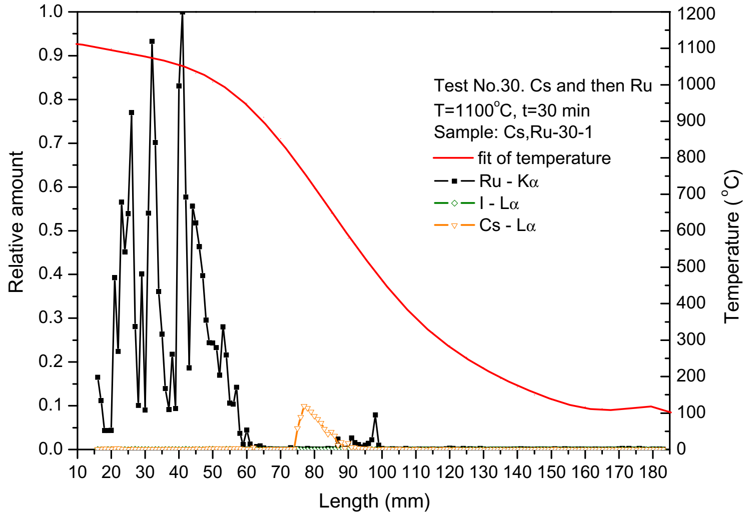

Fig. 13. Axial distribution of deposited elements on quartz rod (sample: Cs-30-1).

4. Conclusions

In the RUSET programme Ru oxidation rate and content of Ru in escaping air flow have been studied with special emphasis on effects of other fission product elements on the Ru oxidation and transport.

The results showed that Ru evaporates in form of RuO_3 and RuO_4; both reached saturation concentration in the high temperature area at the given experimental conditions. In the decreasing temperature section of experimental device between about 1100 and 600 °C most of the RuO_3 and RuO_4 (≈95%) decomposed on quartz surfaces and formed RuO_2 crystals; while the partial pressure of RuO_4 in the escaping air was in the range of 10^{-6} bar, far above the value that would be expected from equilibrium. The decomposition of RuO_3 and RuO_4 to RuO_2 is a heterogeneous phase chemical reaction catalyzed efficiently by the inhomogeneity of quartz surface and the formed RuO_2 particles. On the other hand under the given test conditions, the surface catalyzed decomposition process of RuO_x to RuO_2 was not fast enough to follow entirely the equilibrium with the temperature. In the later phase of tests Ru was coming from the deposited RuO_2 by re-evaporation resulting in about 10^{-6} bar partial pressure in the outlet gas.

Other fission products influenced the concentration of RuO_4 in the ambient temperature escaping gas and raised time delays in appearance of its maximum values. The concentration of RuO_4 in the escaping air was enhanced – i.e. the surface catalyzed decomposition of RuO_3 and RuO_4 to RuO_2 was decreased – by

- steam content of air,
- molybdenum oxide vapour in air,
- MoO_3 layer on quartz surfaces,
- and Cs deposition, which partly diffused into the quartz and changed the quartz surface feature.

Caesium seems to be the fission product element, which plays main role in time delay in appearance of maximum concentration of ruthenium oxides in the ambient temperature escaping gas. If Cs was present in the charge, ruthenium escaped from the high temperature region partly in form of caesium compounds and deposited at relative low temperatures (400–900 °C) compared to the pure RuO_2 precipitations. The deposition mechanism in this case is simple condensation, and this process lowered the ruthenium concentration in the outlet air.

In presence of barium and rare earth oxides barium ruthenate and rare earth ruthenates are formed resulting in extended Ru escape from the high temperature area.

Measurements demonstrated the importance of surface quality in the decreasing temperature area on the heterogeneous phase decomposition of ruthenium oxides to RuO_2. In this way molybdenum and caesium depositions in the RCS can play an important role in the surface catalyzed decomposition of ruthenium oxides (RuO_3 and RuO_4) and so on the source term in a hypothetical air ingress accident.

Results of these experiments are concerning on quartz surfaces, and further experimental investigations are required to address various other surfaces (stainless steel, zirconium alloys, ceramics) in the decreasing temperature area that can be encountered in accidental situation. From the above results also can not be excluded any ruthenium trapping effect of caesium deposition in the decreasing temperature area because of significant caesium diffusion into the quartz material.

References

[1] B.R. Bowsher, Prog. Nucl. Energy 20 (1987) 199–233.

[2] H. Kleykamp, Nucl. Technol. 80 (1988) 412–422.

[3] C. Ronneau, J. Cara, A. Rimski-Korsakov, J. Environ. Radioact. 26 (1995) 63–70.

[4] E.H.P. Cordfunke, R.J.M. Konings, E.F. Westrum Jr., J. Nucl. Mater. 167 (1989) 205–212.

[5] C. Mun, L. Cantrel, C. Madic, Nucl. Technol. 156 (2006) 332–346.

[6] A. Auvinen, G. Brillant, N. Davidovich, R. Dickson, G. Ducros, Y. Dutheillet, P. Giordano, M. Kunstar, T. Kärkelä, M. Mladin, Y. Pontillon, C. Séropian, N. Vér, Nucl. Eng. Des. 238 (2008) 3418–3428.

[7] D.S. Cox, C.E.L. Hunt, Z. Liu, N.A. Keller, R.D. Barrand, R.F. O'Connor, F.C. Iglesias, Fission-product releases from UO_2 in air and inert conditions at 1700–2350 K: analysis of the MCE-1 experiment, in: Proceedings of the American Nuclear Society International Topical Meeting on Safety of Thermal Reactors, Portland, Oregon, USA, 21–25 July 1991. Also issued as Atomic Energy of Canada Limited report, AECL-10438.

[8] R.D. Barrand, R.S. Dickson, Z. Liu, D.D. Semeniuk, Release of fission products from CANDU fuel in air, steam and argon atmospheres at 1500–1900°C: The HCE3 experiment, in: Proceedings of the 6th International Conference on CANDU Fuel, Niagara Falls, Ontario, Canada, September 1999, pp. 271–280.

[9] G. Ducros, Y. Pontillon, P.P. Malgouyres, P. Taylor, Y. Dutheillet, Ruthenium release at high temperature from irradiated PWR fuels in various oxidising conditions; main findings from the VERCORS program, in: Proceedings of the International Conference on Nuclear Energy for New Europe 2005, Bled, Slovenia, September 5–8, 2005, SARNET-ST-P40.

[10] U. Backman, M. Lipponen, A. Auvinen, U. Tapper, R. Zilliacus, J.K. Jokiniemi, Radiochim. Acta 93 (2005) 297–304.

[11] T. Kärkelä, U. Backman, A. Auvinen, R. Zilliacus, M. Lipponen, T. Kekki, U. Tapper, J. Jokiniemi, Experiments on the Behaviour of Ruthenium in Air ingress Accidents – Final Report, April 2007, SARNET-ST-P58, VTT-R-01252-07.

[12] C. Mun, L. Cantrel, C. Madic, Radiochim. Acta 95 (2007) 643–656.

[13] C. Mun, J.J. Ehrhardt, J. Lambert, C. Madic, Appl. Surf. Sci. 253 (2007) 7613–7621.

[14] C. Mun, L. Cantrel, C. Madic, Radiochim. Acta 96 (2008) 375–384.

[15] C. Mun, L. Cantrel, C. Madic, Nucl. Technol. 164 (2008) 245–254.

[16] H. Albrecht, Freisetzung von Spalt- und Aktivierungsprodukten beim LWR-Kernschmelzen, Abschlussbericht des SASCHA-Programmes, KfK 4264, 1987.

[17] R.P. Larsen, L.E. Ross, Anal. Chem. 31 (1959) 176–178.

[18] J.I. Bramman, R.M. Sharpe, D. Thom, G. Yates, J. Nucl. Mater. 25 (1968) 201–215.

[19] C.H. Lee, M.Y. Suh, K.S. Choi, et al., Anal. Chim. Acta 475 (2003) 171–179.

[20] E.H.P. Cordfunke, R.J.M. Konings, Saskia R.M. Meyssen, J. Chem. Thermodyn. 24 (1992) 725–728.

[21] H. Schäfer, A. Tebben, W. Gerhardt, Z. Anorg. Allg. Chem. 321 (1963) 41–55.

[22] Wayne E. Bell, M. Tagami, J. Phys. Chem. 67 (1963) 2432–2436.

[23] T. Kärkelä, U. Backman, A. Auvinen, R. Zilliacus, M. Lipponen, T. Kekki, U. Tapper, J. Jokiniemi, Experiments on the Behaviour of Ruthenium in Air Ingress Accidents – Progress Report, Electronic report, February 2006, NKS-118, ISBN 87-7893-179-7.

[24] J. Berkowitz, M.G. Inghram, W.A. Chupka, J. Chem. Phys. 26 (1957) 842–846.

[25] J.C.J. Bart, G. Petrini, N. Giordano, Z. Anorg. Allg. Chem. 412 (1975) 258–270.